

## Research Paper

# Estrogen-related receptor alpha is involved in Alzheimer's disease-like pathology

Ying Tang<sup>a,1</sup>, Zhuo Min<sup>a,1</sup>, Xiao-Jiao Xiang<sup>a</sup>, Lu Liu<sup>c</sup>, Yuan-Lin Ma<sup>a</sup>, Bing-Lin Zhu<sup>a</sup>, Li Song<sup>a</sup>, Jing Tang<sup>a</sup>, Xiao-Juan Deng<sup>a</sup>, Zhen Yan<sup>b</sup>, Guo-Jun Chen<sup>a,\*</sup>

<sup>a</sup> Department of Neurology, the First Affiliated Hospital of Chongqing Medical University, Chongqing Key Laboratory of Neurology, 1 Youyi Road, Chongqing 400016, China

<sup>b</sup> Department of Physiology and Biophysics, State University of New York at Buffalo, Buffalo, NY 14214, USA

<sup>c</sup> Thirteenth people's Hospital of Chongqing, Chongqing 400016, China

## ARTICLE INFO

## Keywords:

Estrogen-related receptor  $\alpha$   
APP/PS1 mice  
Amyloidogenesis  
Tau phosphorylation

## ABSTRACT

Estrogen-related receptor alpha (ERR $\alpha$ ) is a transcriptional factor associated with mitochondrial biogenesis and energy metabolism. However, little is known about the role of ERR $\alpha$  in Alzheimer's disease (AD). Here, we report that in APP/PS1 mice, an animal model of AD, ERR $\alpha$  protein and mRNA were decreased in a region- and age-dependent manner. In HEK293 cells that stably express human full-length  $\beta$ -amyloid precursor protein (APP), overexpression of ERR $\alpha$  inhibited the amyloidogenic processing of APP and consequently reduced A $\beta_{1-40/1-42}$  level. ERR $\alpha$  overexpression also attenuated Tau phosphorylation at selective sites, with the concomitant reduction of glycogen synthase kinase 3 $\beta$  (GSK3 $\beta$ ) activity. Interestingly, alterations of APP processing and Tau phosphorylation induced by hydrogen peroxide were reversed by ERR $\alpha$  overexpression in HEK/APP cells. These results indicated that ERR $\alpha$  plays a functional role in AD pathology. By attenuating both amyloidogenesis and Tau phosphorylation, ERR $\alpha$  may serve as a potential therapeutic target for AD.

## 1. Introduction

Alzheimer's disease (AD) is the most common form of neurodegenerative dementia in the elderly (El Kadmiri et al., 2017). It is estimated that about 24.3 million people had dementia in 2005, with 4.6 million new cases per year, the number of people will double every 20 years, leading to 81.1 million by 2040 (Ferri et al., 2005). The pathological hallmarks of AD are amyloid protein (A $\beta$ ) deposition and neurofibrillary tangles (NFTs) (Querfurth and LaFerla, 2010). Although many clinical and experimental studies are ongoing, achieving a cure by simply targeting A $\beta$  or NFTs has proven to be difficult (Mangialasche et al., 2010). Hence, it may be more relevant to identify multifunctional molecules that affect both A $\beta$  generation and NFTs.

Estrogen-related receptor  $\alpha$  (ERR $\alpha$ ) is a member of orphan nuclear receptor transcription factors, with no known endogenous ligand (Huss et al., 2015). Accumulating evidence has suggested that ERR $\alpha$  plays a central role in regulating gene expression related to mitochondrial

biogenesis, oxidative phosphorylation, glycolysis and fatty acid metabolism (Audet-Walsh and Giguere, 2015; Giguere, 2008; Huss et al., 2015; Mootha et al., 2003; Ranhotra, 2015a, 2015b). ERR $\alpha$  also exerts anti-inflammatory activities by regulating gene expression (Yuk et al., 2015). Interestingly, neuroinflammation and oxidative stress are closely associated with AD pathogenesis including A $\beta$  generation and tau-hyperphosphorylation (Jakob-Roetne and Jacobsen, 2009; Querfurth and LaFerla, 2010). It is reported that ERR $\alpha$  has a broad expression in the brain and is regulated by energy status (Cui et al., 2015; Gofflot et al., 2007). On the other hand, reduced energy metabolism in the brain is strongly related to clinical dementia (Jakob-Roetne and Jacobsen, 2009).

We hypothesized that the expression of ERR $\alpha$  in the brain of AD may be altered; and ERR $\alpha$  is functionally associated with AD-like pathogenesis. In this study, we used APP/PS1 mice as an AD model. This model harbors the Swedish mutation (K670N/M671L) of human APP and the mutant presenilin-1 (PS1) gene. Animals develop

**Abbreviations:** A $\beta$ , amyloid protein; AD, Alzheimer's disease; ADAM10, a disintegrin and metalloproteinase 10; AMPK, AMP-activated protein kinase; APP,  $\beta$ -amyloid precursor protein; APP/PS1, expressing Swedish APP and Presenilin1 delta exon 9 mutations; BACE1,  $\beta$ -amyloid converting enzyme 1;  $\beta$ -CTF,  $\beta$ -COOH-terminal fragment; ERR $\alpha$ , estrogen-related receptor alpha; ERR $\gamma$ , estrogen-related receptor gamma; HEK/APP, HEK293 cells stably expressing human full-length APP; GSK3 $\beta$ , glycogen synthase kinase 3 $\beta$ ; MPP<sup>+</sup>, *N*-methyl-4-phenylpyridiniumion; NFTs, neurofibrillary tangles; PPAR $\gamma$ , Peroxisome proliferator-activated receptor  $\gamma$ ; shRNA, Short hairpin RNA; WT, wild-type

\* Corresponding author.

E-mail address: [woodchen2015@163.com](mailto:woodchen2015@163.com) (G.-J. Chen).

<sup>1</sup> Ying Tang and Zhuo Min contributed equally to this work.

<https://doi.org/10.1016/j.expneurol.2018.04.003>

Received 22 November 2017; Received in revised form 28 March 2018; Accepted 6 April 2018

Available online 08 April 2018

0014-4886/ © 2018 Published by Elsevier Inc.

amyloidogenesis and Tau-positive neuritis, resembling AD-like pathologies in patients (Bilkei-Gorzo, 2014). In APP/PS1 mice, we assessed the expression of  $ERR\alpha$  in the cortex and hippocampus, at 6 mon, 12 mon and 18 mon, respectively. In a cellular model that stably expresses human full-length APP, we assessed the effect of  $ERR\alpha$  on A $\beta$  generation and Tau phosphorylation in normal condition and in oxidative stress.

## 2. Materials and methods

### 2.1. Animal models

APP/PS1 mice expressing Swedish APP and Presenilin1 delta exon 9 mutations (B6C3-Tg (APP<sup>swe</sup>, PSEN1<sup>dE9</sup>) 85Dbo/J, # 004462) were purchased from the Model Animal Research Centre of Nanjing University and were maintained in the Experimental Animal Center of Chongqing Medical University. Food and water were available ad libitum. All of the animal procedures conformed to the Ethics Committee of Chongqing Medical University.

### 2.2. Antibodies and reagents

Antibodies against  $ERR\alpha$  (ab76228; 1:1000, for Western blotting), ADAM10 (ab1997; 1:1000), BACE1 (ab2077; 1:1000), total-Tau (ab64193; 1:1000), p-TauT231 (ab151559; 1:1000), p-TauS262 (ab131354; 1:1000), p-TauS396 (ab109390; 1:1000), GSK3 $\beta$  (ab93926; 1:1000) and p-GSK3 $\beta$ -Ser9 (ab75814; 1:1000) were purchased from Abcam (Cambridge, United Kingdom). Anti- $ERR\alpha$  (SC-65718; 1:100, for immunostaining) was from Santa Cruz (California, USA); Antibodies against APP and CTFs (A8717; 1:1000) were from Sigma-Aldrich (St. Louis, MO). Primary antibody against GAPDH or MYC (60003–2-Ig; 1:4000) was from Proteintech (Wuhan, China) and horseradish peroxidase-conjugated anti-rabbit or anti-mouse secondary antibodies were purchased from Proteintech (Wuhan, China). Immunohistochemistry experiment was performed with Goat hypersensitive two-step detection kit (PV-9003, ZSGB-BIO, Beijing, China).

### 2.3. Cell culture, plasmid and short hairpin RNA (shRNA) transfection

Human embryonic kidney 293 cell line (HEK293) stably expressing full-length human APP (HEK/APP), was generated as described previously (Hu et al., 2017). The human *ESRR*A plasmid (HG15911-CM) and control vector pCMV3 (CV013) were purchased from Sino Biological (Beijing, China). Cells were transfected with Lipofectamine™ 2000 Transfection Reagent (11668019, Thermo Fisher Scientific, Inc) and with Opti-MEM Reduced Serum Media (Thermo Fisher Scientific, Inc) according to manufacturer's protocol. The shRNA sequence for human *ESRR*A (5'-GTGAATGCACTGGTGTCTCAT-3') was selected from Invitrogen Block-iT RNAi Designer. This sequence was synthesized by Sangon Biotech (Shanghai, China) and designed as follows: 5'-GATC CCC GTGAATGCACTGGTGTCTCAT TTCAAGAGA ATGAGACACCAGTGCATTAC TTTTT-3' (sense); and 5'-AGCTAAAAA GTGAATGCACTGGTGTCTCAT TCTCTTAA ATGAGACACCAGTGCATTAC GGG-3' (antisense). These sequences were first annealed and subsequently cloned into pSUPER RNAi empty vector provided by Key Laboratory of Mental Health, Ministry of Health (Peking University). The annealing reaction mixture (50  $\mu$ l in total) consisted of both of the forward and reverse oligonucleotides, 5  $\mu$ l 10  $\times$  LA Taq buffer Mg<sup>+</sup> free (9153 AM, Takara, Dalian, China) and ddH<sub>2</sub>O. The annealing temperature was at 95 °C for 5 min, followed by 70 °C for 10 min before cooling down at room temperature. The pSUPER empty vector was cut in the 50  $\mu$ l mixture of 2  $\mu$ l *Hind*III (FD0504, Thermo Fisher Scientific, Inc), 2  $\mu$ l *Bgl*II FastDigest restriction endonuclease (FD0083, Thermo Fisher Scientific, Inc), 5  $\mu$ l FastDigest buffer, 5  $\mu$ g pSUPER plasmid and ddH<sub>2</sub>O, at 37 °C for 30 min. Digested empty vector was verified by agarose gel electrophoresis and purified using Gel Extraction Kit (D2500-01, Omega,

Norcross, GA). Empty vector and target nucleotides were linked in the reaction mixture (15  $\mu$ l) composed of 1.5  $\mu$ l 10  $\times$  ligase buffer, 1  $\mu$ l digested empty vector, 5  $\mu$ l double stranded nucleotides, 1  $\mu$ l T4 ligase (C301-01-AB, Vazyme, Nanjing, China), and 6.5  $\mu$ l ddH<sub>2</sub>O at 4 °C overnight. The final products were subsequently processed through transformation and colony PCR as described previously (Bergkessel and Guthrie, 2013).

### 2.4. Western blotting analysis

APP/PS1 mice and wild-type littermate at different age were first euthanized and then the brain was harvested immediately. The cortex and hippocampus on both sides were isolated. Proteins were extracted using RIPA buffer supplemented with protease inhibitors and phosphatase inhibitors (Byotime, Haimen, China) mixture and centrifuged at 12,000 rpm for 15 min at 4 °C. Protein concentrations were measured using a BCA Protein Assay Kit (P0011, Byotime, Haimen, China) and Western blotting were performed as previously described (Hu et al., 2017; Liu et al., 2017). The specific protein bands were visualized using ECL reagent (GE healthcare, UK) and the Fusion FX5 image analysis system (Vilber Lourmat, Marne-la-Vallee, France). Relative protein expression levels were calculated by Quantity One software (Bio-Rad, Hercules, CA) normalized to GAPDH or  $\beta$ -actin.

### 2.5. Immunohistochemistry

Brain slices from mice (18-month-old) were paraffin-embed and deparaffinized in xylene for 30 min, and were rehydrated in a series concentration of ethanol for a few minutes. After washing with phosphate-buffered saline (PBS, 5 min  $\times$  3), brain slices were permeabilized with 0.4% Triton-X 100 for 20 min before antigen retrieval with boiled sodium citrate buffer (10 mM, pH 6.0) for about 15 min, followed by PBS washing and incubation with 3% H<sub>2</sub>O<sub>2</sub> (PV-9003, ZSGB-BIO, Beijing, China) for 15 min at 37 °C. Slices were incubated with anti- $ERR\alpha$  antibody overnight at 4 °C. Brain tissues were washed and incubated with reaction enhancement solution (PV-9003, ZSGB-BIO, Beijing, China) for 30 min at 37 °C and with enhanced enzyme-labeled rabbit anti-goat IgG polymer (PV-9003, ZSGB-BIO, Beijing, China) for 30 min at 37 °C. Slices were then treated with 3,3'-diaminobenzidine (DAB, ZSGB-BIO, Beijing, China) for 2 min and PBS. Hematoxylin was used to counterstain nuclei for several minutes. Slices were dehydrated by lithium carbonate for 1 min and incubated with dimethylbenzene for 40 min, then covered and dried overnight. Quantification of immunohistochemistry was calculated by Image-pro Plus 6.0 software (Media Cybernetics, Bethesda, USA) as described previously (Liu et al., 2017).

### 2.6. RNA extraction and quantitative RT-PCR

Total RNA was extracted from mice brain tissue lysed by using RNAiso plus (Takara, Dalian, China). The cDNA was synthesized by the 5  $\times$  HiScript II Select qRT Super Mix II (R233-01-AC, Vazyme, Nanjing, China) according to manufacturer's protocol. mRNA expression levels of  $ERR\alpha$  and  $\beta$ -actin were detected by RT-qPCR. The primers for mice  $ERR\alpha$  and  $\beta$ -actin were as follows:  $ERR\alpha$ , 5'-AGCAAGCCCCGATGGA-3', and antisense: 5'-GAGAGGCCTGGGATGCTCTT-3'; and  $\beta$ -actin, sense: 5'-ACGGTCAGGTCATCACTATCG-3', and antisense: 5'-GGCATAGAGGTCTTTACGGATG-3'. Reactions were performed with AceQ qPCR SYBR Green Master Mix (Q111-02, Vazyme, Nanjing, China). The reaction mixture (20  $\mu$ l total) consisted of 10  $\mu$ l SYBR, 5.2  $\mu$ l nuclease-free water, 0.4  $\mu$ l each primer, and 4  $\mu$ l diluted cDNA. Reactions were performed using the following steps: 95 °C for 5 min, followed by 40 cycles of 95 °C for 10 s and 60 °C for 30 s, and the melting curve was run after RT-PCR. The Ct value of each sample was recorded as previously described (Zhu et al., 2016).

## 2.7. ELISA for $A\beta_{1-40}$ and $A\beta_{1-42}$

Human  $A\beta_{1-40}$  and  $A\beta_{1-42}$  levels in cultured HEK/APP cells were measured using ELISA kits (Cusabio, China). As  $A\beta$  was secreted in the conditioned media, supernatant of cultured media was collected and centrifuged for 10 min at 4000 g at 4 °C. All samples were assayed in 3 duplicates, and each experiment was repeated 3 times.

## 2.8. Statistical analysis

Data were presented as mean  $\pm$  standard error and analyzed using GraphPad Prism version 7.0 (GraphPad Software, La Jolla, CA, USA) by unpaired independent student's *t*-test, one-way ANOVA and two-way ANOVA where it applied.

## 3. Results

### 3.1. Cerebral ERR $\alpha$ protein was decreased in APP/PS1 mice

To determine whether ERR $\alpha$  may be involved in the pathophysiology of AD, we first assessed ERR $\alpha$  protein level in the cortex and hippocampus of APP/PS1 mice (APP/PS1) relative to those in wild-type mice (WT). Three different ages: 6 mon (young), 12 mon (mid-aged) and 18 mon (old) were chosen for comparisons. As shown in Fig. 1A, in the cortex, ERR $\alpha$  protein was decreased by at least 0.5-fold in APP/PS1 mice at 6 mon, 12 mon and 18 mon, respectively, compared with WT. In the hippocampus, ERR $\alpha$  was not different in APP/PS1 mice at 6 mon and 12 mon, while a significantly low level was found in 18 mon

(Fig. 1B). To further validate that ERR $\alpha$  protein was decreased in APP/PS1 mice by Western blotting, we performed immunohistochemical staining to assess ERR $\alpha$  expression in hippocampal CA1 and CA3 areas and the cortex in 18-mon-old mice, using another anti-ERR $\alpha$  antibody. As shown in Fig. 2A, ERR $\alpha$  was mainly localized in the nucleus. The density of ERR $\alpha$  was significantly decreased in CA1, CA3 and cortex of APP/PS1 mice, compared with WT (Fig. 2B). These results indicated that while cortical ERR $\alpha$  was decreased in APP/PS1 mice regardless of age, hippocampal ERR $\alpha$  did not change until late stage (18 mon).

### 3.2. ERR $\alpha$ mRNA was age-dependently decreased in the hippocampus of APP/PS1 mice

To further identify whether the decreased protein of ERR $\alpha$  was associated with transcriptional regulation, we assessed ERR $\alpha$  mRNA in APP/PS1 and WT mice with different ages using qPCR. Unexpectedly, in the cortex, ERR $\alpha$  mRNA was not changed at 6 mon, 12 mon and 18 mon in APP/PS1 mice relative to WT (Fig. 3A). In the hippocampus, ERR $\alpha$  was not altered at 6 mon and 12 mon in APP/PS1 mice relative to WT (Fig. 3B). However, significantly decreased ERR $\alpha$  transcripts were found in 18 mon APP/PS1 mice. These results indicated that while cortical ERR $\alpha$  mRNA did not change in APP/PS1 mice, hippocampal ERR $\alpha$  mRNA was downregulated only in 18 mon APP/PS1 mice.

### 3.3. ERR $\alpha$ affected APP processing and tau phosphorylation in HEK/APP cells under basal condition

The altered ERR $\alpha$  expression in APP/PS1 mice prompted us to

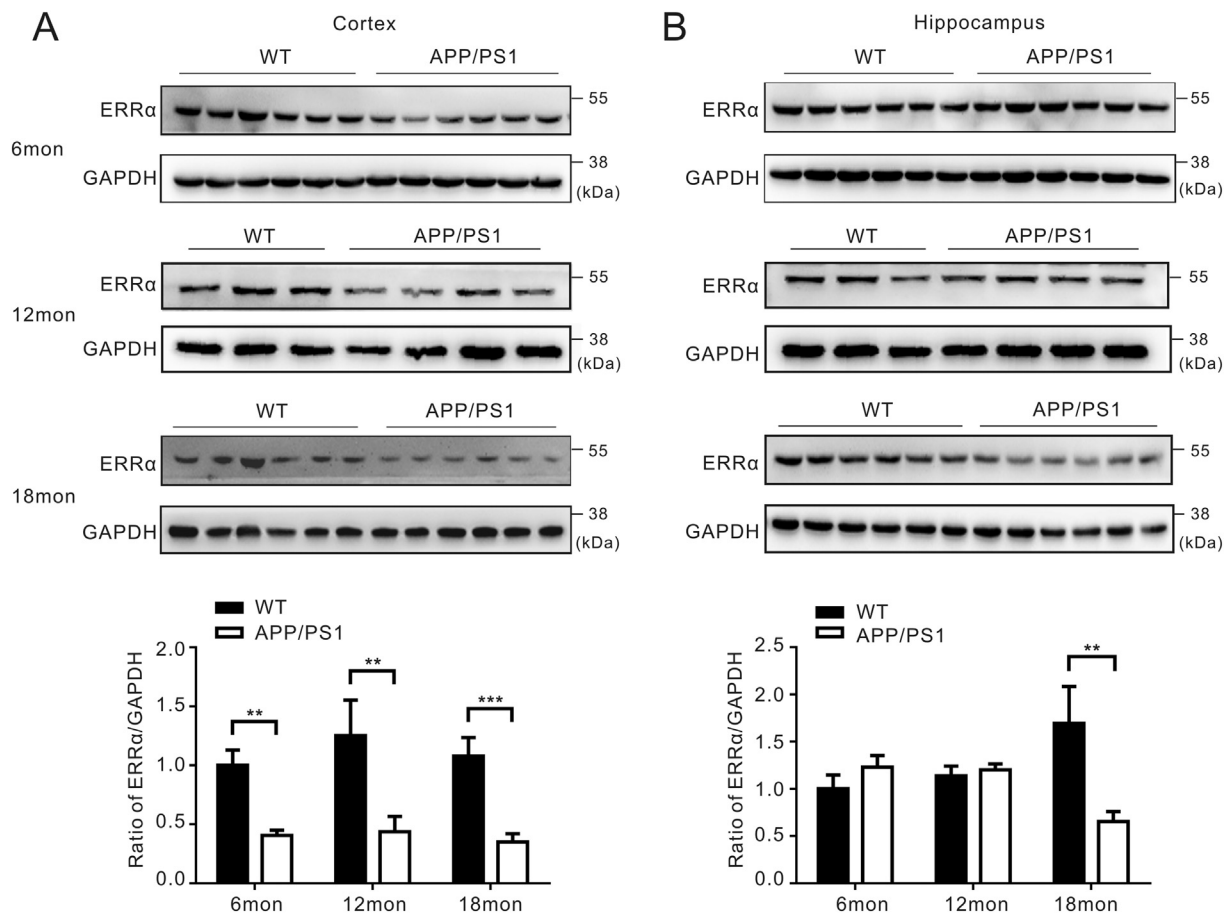


**Fig. 1.** ERR $\alpha$  protein is reduced in the cortex and hippocampus of APP/PS1 mice in an age-dependent manner. (A) Western Blots and bar plot summary of ERR $\alpha$  protein in the cortex of wild-type (WT) and APP/PS1 mice, at 6 mon ( $n = 6$  in each group), 12 mon ( $n = 3$  in WT,  $n = 4$  in APP/PS1) and 18 mon ( $n = 6$  in each group), respectively. (B) Western Blots and bar plot summary of ERR $\alpha$  protein in the hippocampus of WT and APP/PS1 mice, at 6 mon ( $n = 6$  in each group), 12 mon ( $n = 3$  in WT,  $n = 4$  in APP/PS1) and 18 mon ( $n = 6$  in each group), respectively. \*\* $p < 0.01$ , \*\*\* $p < 0.001$ .

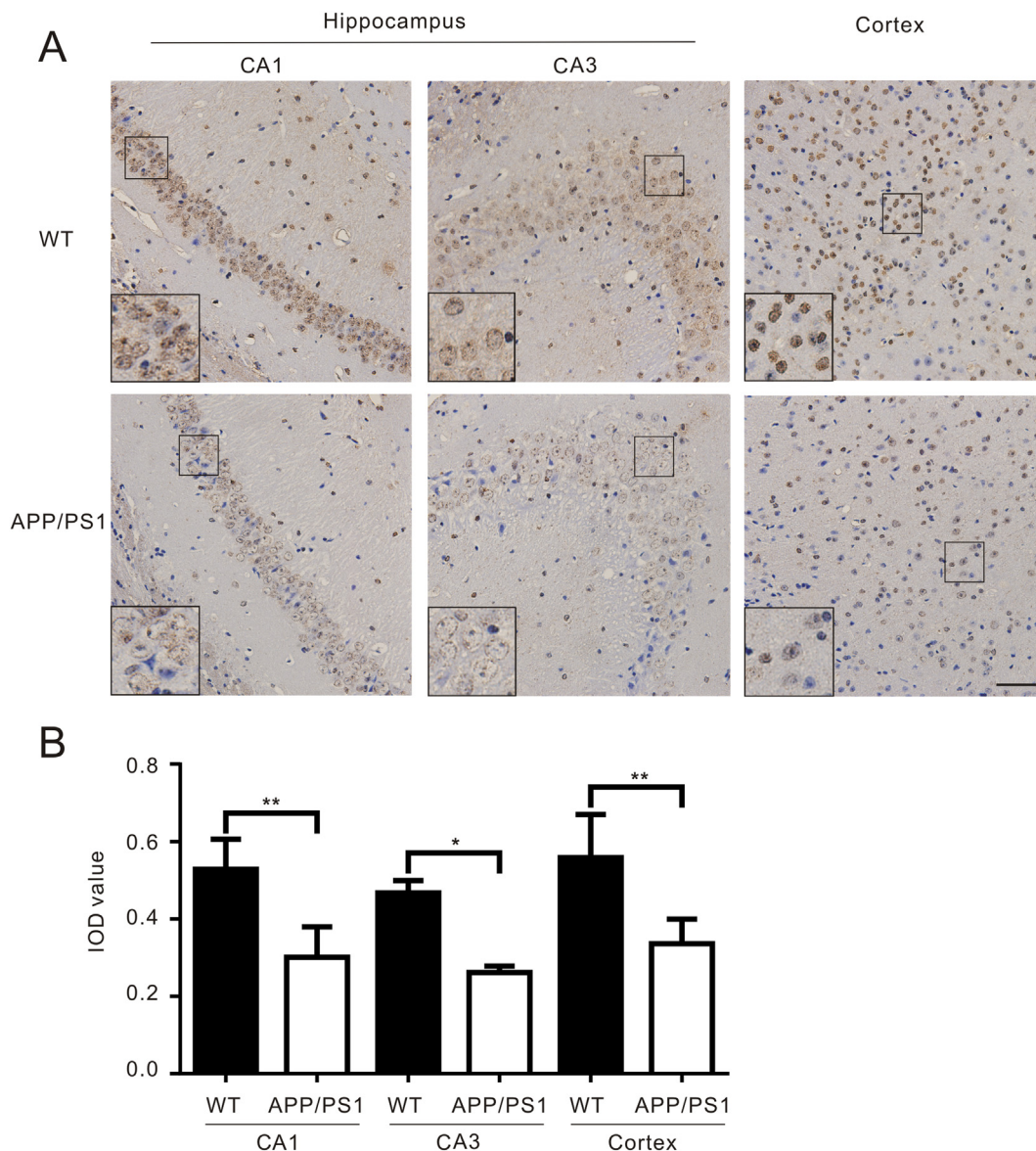


**Fig. 2.** ERR $\alpha$  immunoreactivity is decreased in the hippocampus and cortex of APP/PS1 mice at 18 mon. **(A)** Representative immunohistochemical images probed by ERR $\alpha$  antibody in neurons of CA1/CA3 area of the hippocampus (left two columns) and the cortex (right column). Samples were taken from WT (n = 4) and APP/PS1 mice (n = 4), respectively. Compared with WT, APP/PS1 shows reduced ERR $\alpha$  immunoreactivity in the hippocampus and the cortex. Scale bar = 50  $\mu$ m. **(B)** Bar plot summary of IOD (integrated optic density) of ERR $\alpha$  in CA1/CA3 and the cortex, from WT and APP/PS1, respectively. \*p < 0.05, \*\*p < 0.01, n = 4 in each group.

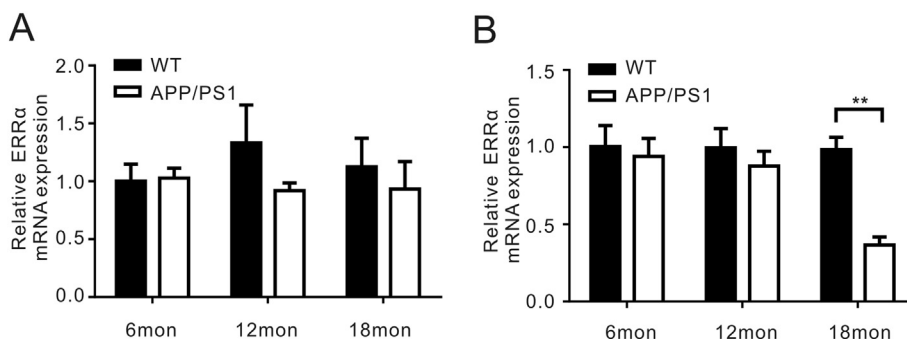


**Fig. 3.** ERR $\alpha$  transcripts are decreased only in the hippocampus of APP/PS1 mice at 18 mon. **(A)** Relative ERR $\alpha$  mRNA levels in the cortex of WT and APP/PS1 mice at 6 mon, 12 mon and 18 mon, respectively (n = 6 in each group). **(B)** Relative ERR $\alpha$  mRNA levels in the hippocampus of WT and APP/PS1 mice at 6 mon, 12 mon and 18 mon, respectively (n = 6 in each group). The quantitative expression was calculated using the  $2^{-\Delta\Delta Ct}$  method.  $\beta$ -actin was used as internal control. \*\*p < 0.01.

speculate that ERR $\alpha$  might be involved in AD-associated pathology. It is reported that A $\beta$  deposition and Tau hyper-phosphorylation play a key role in pathogenesis of AD (Ballard et al., 2011). A $\beta$  is generated from  $\beta$ -amyloid precursor protein (APP) through enzymatic proteolysis. The amyloidogenic cleavage of APP is mediated by  $\beta$ -amyloid converting

enzyme 1(BACE1), resulting in increased  $\beta$ -COOH-terminal fragment ( $\beta$ -CTF) (Singer et al., 2005). In contrast, ADAM10 (a disintegrin and metalloproteinase 10) promotes the non-amyloidogenic cleavage of APP, resulting in the increased generation of  $\alpha$ -CTF and the reduced A $\beta$  (Postina, 2012). Thus, we first assessed the effect of ERR $\alpha$

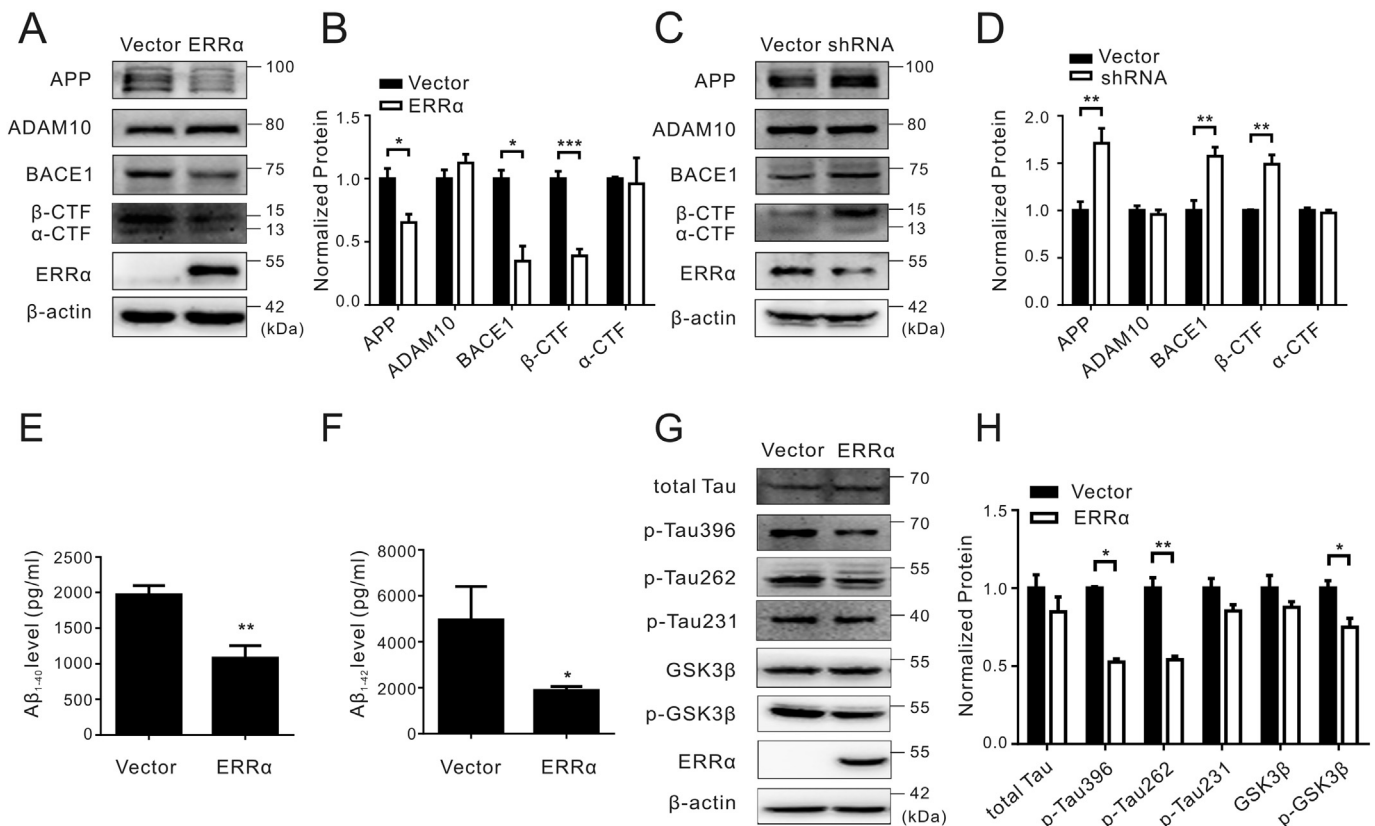


**Fig. 4.** ERRα affects APP processing and Tau phosphorylation under normal condition. (A&B) Representative Western blots (A) and bar plot summary (B) of APP, BACE1, ADAM10 and  $\alpha$ -,  $\beta$ -CTF in HEK/APP cells transfected with Vector or ERRα for 48 h. (C&D) Representative Western blots (A) and bar plot summary (B) of APP, BACE1, ADAM10 and  $\alpha$ -,  $\beta$ -CTF in HEK/APP cells transfected with Vector or ERRα shRNA for 48 h. (E&F) Protein levels of A $\beta$ <sub>1-40</sub> (E) and A $\beta$ <sub>1-42</sub> (F) in culture medium from HEK/APP cells transfected with ERRα for 48 h, using corresponding ELISA kits. Absorbance was detected at 450 nm. (G&H) Representative Western blots (G) and bar plot summary (H) of total-Tau, p-Tau396, p-Tau231, p-Tau262, GSK3 $\beta$  and p-GSK3 $\beta$  in HEK/APP cells transfected with Vector or ERRα for 48 h. \* $p < 0.05$ , \*\* $p < 0.01$ , \*\*\* $p < 0.001$ ,  $n = 3$  in each group.

overexpression on APP processing. As shown in Fig. 4A&B, ERRα overexpressing cells showed a significant reduction of APP, BACE1 and  $\beta$ -CTF, while ADAM10 and associated  $\alpha$ -CTF were not significantly altered. To further validate that ERRα controlled APP processing, we assessed APP processing in HEK/APP cells transiently transfected with ERRα shRNA. Compared to control, knockdown of ERRα significantly increased protein levels of APP, BACE1 and  $\beta$ -CTF, whereas those of ADAM10 and  $\alpha$ -CTF were not significantly altered (Fig. 4C&D). Accordingly, both A $\beta$ <sub>1-40</sub> and A $\beta$ <sub>1-42</sub> were significantly reduced in HEK/APP cells that overexpressed ERRα.

The deregulation of several phosphorylated sites of Tau, such as Ser262, Thr231, and Ser396 is closely associated with AD (Lee and Leurgers, 2012). It is also reported that GSK3 $\beta$ , a key enzyme in Tau phosphorylation, plays a critical role in AD pathogenesis (Billingsley and Kincaid, 1997). We next assessed the effect of ERRα on Tau phosphorylation in HEK/APP cells overexpressing ERRα. As shown in Fig. 4E&F, overexpression of ERRα in HEK/APP cells displayed a decrease of p-Tau396, p-Tau262 and p-GSK3 $\beta$ -S9 relative to vehicle control. In addition, while total level of GSK3 $\beta$  was not altered, p-GSK3 $\beta$  was significantly decreased in ERRα overexpressing cells. These results indicated that in addition to APP processing, Tau phosphorylation and related GSK3 $\beta$  activity were also affected by ERRα.

### 3.4. ERRα also attenuated AD-like pathology under oxidative stress

Mitochondrial dysfunction and oxidative stress are closely associated with AD pathogenesis (Jakob-Roetne and Jacobsen, 2009; Querfurth and LaFerla, 2010; Sheng et al., 2012). Interestingly, ERRα plays a key role in neuroprotection through its antioxidant activities

(Banse et al., 2015; Hyatt et al., 2016; Lim et al., 2012; Rangwala et al., 2007; Zhou et al., 2014). It may be important to identify whether ERRα affects AD-like pathology in oxidative environment. Thus, we assessed APP processing and Tau phosphorylation in HEK/APP cells treated with 50  $\mu$ M H<sub>2</sub>O<sub>2</sub> for 24 h. As shown in Fig. 5A, H<sub>2</sub>O<sub>2</sub> treatment caused significant increase of APP and BACE1 and significant decrease of ADAM10 protein, with concomitant alteration of  $\alpha$ - and  $\beta$ -CTF (Fig. 5A &B), indicating that oxidative stress affected APP processing (Azmi et al., 2015; Nagai et al., 2017). Transfection of ERRα in H<sub>2</sub>O<sub>2</sub> treated HEK/APP cells resulted in the reduction of APP and BACE1. Interestingly, ERRα increased ADAM10 in H<sub>2</sub>O<sub>2</sub> treated cells compared with vehicle. Although there were trends towards decreased  $\beta$ -CTF and increased  $\alpha$ -CTF in ERRα overexpressing cells, they were not significant (Fig. 5A&B).

It is reported that H<sub>2</sub>O<sub>2</sub> also altered Tau phosphorylation (Feng et al., 2013). Consistently, we found that in HEK/APP cells treated with H<sub>2</sub>O<sub>2</sub>, p-Tau396, p-Tau262 and p-Tau231 were all increased; with total Tau protein level unaffected (Fig. 5C&D). This effect was further reversed in cells overexpressing ERRα (Fig. 5C&D). Accordingly, while H<sub>2</sub>O<sub>2</sub> did not cause alteration of total level of GSK3 $\beta$  protein, p-GSK3 $\beta$  was significantly increased. In H<sub>2</sub>O<sub>2</sub> treated cells, overexpression of ERRα led to a significant reduction of p-GSK3 $\beta$  (Fig. 5C&D). These results indicated that ERRα reversed the elevated amyloidogenic APP processing and Tau phosphorylation in cells under oxidative stress.

## 4. Discussion

ERRα is expressed in a variety of tissues, including the brain (Ranhotra, 2009; Tarrant et al., 2006). It is reported that long-term

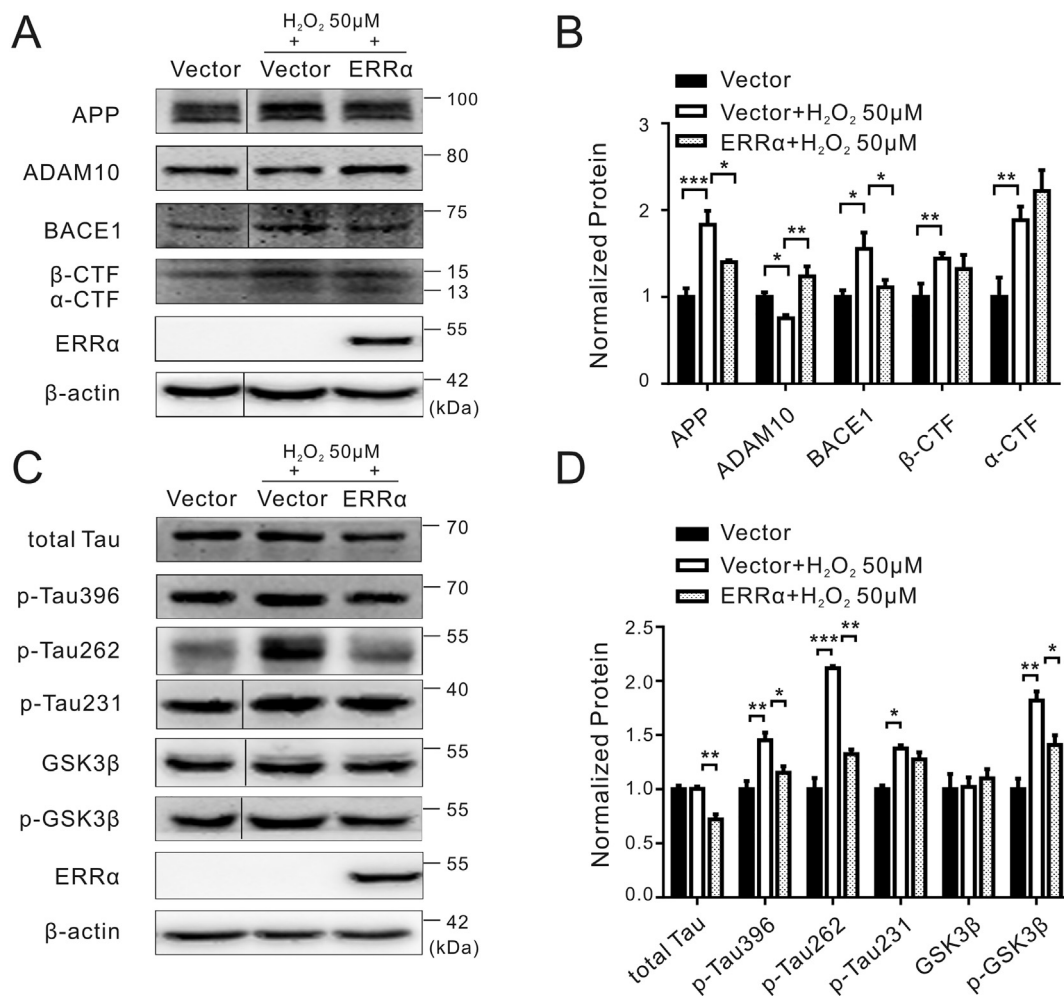


**Fig. 5.** Overexpression of ERR $\alpha$  attenuates AD-like pathology in oxidative stress. **(A)** Representative Western blots of APP, BACE1, ADAM10 and  $\alpha$ - and  $\beta$ -CTF in HEK/APP cells transiently transfected with Vector or ERR $\alpha$  for 48 h. 50  $\mu$ M H<sub>2</sub>O<sub>2</sub> was added for 24 h before samples were collected. **(B)** Quantitative analysis of proteins shown in panel A in HEK/APP cells transiently transfected with vector alone (Vector), or vector/ERR $\alpha$  construct treated with 50  $\mu$ M H<sub>2</sub>O<sub>2</sub> (Vector + 50  $\mu$ M H<sub>2</sub>O<sub>2</sub>/ERR $\alpha$  + 50  $\mu$ M H<sub>2</sub>O<sub>2</sub>). **(C)** Representative Western blots of total-Tau, p-Tau396, p-Tau231, p-Tau262, GSK3 $\beta$  and p-GSK3 $\beta$  in HEK/APP cells transiently transfected with ERR $\alpha$  or Vector for 48 h. with Vector or ERR $\alpha$  for 48 h. 50  $\mu$ M H<sub>2</sub>O<sub>2</sub> was added for 24 h before samples were collected. **(D)** Quantitative analysis of proteins shown in panel C in HEK/APP cells transiently transfected with vector alone (Vector), or vector/ERR $\alpha$  construct treated with 50  $\mu$ M H<sub>2</sub>O<sub>2</sub> (Vector + 50  $\mu$ M H<sub>2</sub>O<sub>2</sub>/ERR $\alpha$  + 50  $\mu$ M H<sub>2</sub>O<sub>2</sub>). \* $p$  < 0.05, \*\* $p$  < 0.01, \*\*\* $p$  < 0.001,  $n$  = 3 in each group.

caloric restriction results in increased ERR $\alpha$  protein in peripheral tissues including the heart but not in the brain (Ranhotra, 2009). Rosiglitazone can increase ERR $\alpha$  mRNA in the brain (Strum et al., 2007). In SH-SY5Y cells, an oxidative drug *N*-methyl-4-phenylpyridinium ion (MPP<sup>+</sup>) is shown to reduce ERR $\alpha$  protein (Ye et al., 2017). Dysfunction of ERR $\alpha$  may be associated with neurological diseases. For instance, in a mouse model of cerebral ischemia, ERR $\alpha$  protein is increased (Choi et al., 2016). ERR $\alpha$  gene mutation increases the risk of developing eating disorder (Cui et al., 2013). Cerebral knockdown of ERR $\alpha$  impairs behavioral performances in mice (Cui et al., 2015). To the best of our knowledge, no previous study has demonstrated that ERR $\alpha$  expression is associated with AD.

The present study reveals that in the cortex, ERR $\alpha$  is reduced at protein but not mRNA level, regardless of age. In the hippocampus, the reduction of ERR $\alpha$  protein and mRNA occurs only in aged mice. Although ERR $\alpha$  target genes have been intensively investigated (Audet-walsh and Giguère, 2014), how ERR $\alpha$  itself is regulated in the brain remains unclear. It may be unlikely that the region-dependent alteration of ERR $\alpha$  is caused by distinct distribution of A $\beta$  load, as APP/PS1 mice develop cerebral amyloidosis (A $\beta$  deposition) as early as 6–8 weeks in both cortex and hippocampus, which exists throughout life span (Bilkei-Gorzo, 2014; Webster et al., 2014). The selected

reduction of ERR $\alpha$  protein but not mRNA in the cortex might suggest a post-transcriptional mechanism, which remains to be clarified in the future. In the hippocampus, the age-dependent reduction of ERR $\alpha$  protein and mRNA may imply an involvement of energy metabolism or oxidative stress. The hippocampus has enhanced energy demand and mitochondrial stress relative to the cortex (Cabre et al., 2016). As described above, rosiglitazone is able to regulate ERR $\alpha$  mRNA (Strum et al., 2007), which involves peroxisome proliferator-activated receptor  $\gamma$  (PPAR $\gamma$ ) signaling in energy metabolism (Wang et al., 2016). Evidence also suggests that oxidative stress is one of the prominent features in hippocampal aging (Blalock et al., 2003). Whether these mechanisms are involved in the differentially expressed ERR $\alpha$  is currently unknown.

The current study provides evidence that ERR $\alpha$  reduces A $\beta$  generation in HEK/APP cells (Fig. 4E&F), suggesting an important role of ERR $\alpha$  in AD-like pathology. A $\beta$  generation is closely related to the function of BACE1 and ADAM10 (Endres and Fahrenholz, 2012; Pimplikar, 2009; Yan et al., 2016). In line with this, our results also show BACE1 protein is reduced in ERR $\alpha$  overexpressing cells in control condition and oxidative stress. BACE1 expression can be regulated by PPAR $\gamma$  and oxidative stress (Cao et al., 2016; Chami and Checler, 2012; Ly et al., 2013; Tamagno et al., 2002). Interestingly, ERR $\alpha$  may use the

similar mechanisms to regulate BACE1. It is reported that ERR $\alpha$  is a key transcription factor directly regulating PPAR family (Giguere, 2008; Huss and Kelly, 2004; Mistry and Cresci, 2010). Moreover, ERR $\alpha$  protects cells against oxidative damage by promoting the expression of detoxifying enzymes including superoxide dismutase 2 (SOD2) and glutathione S-transferase MU-1 (GSTM1) (Deblois et al., 2009; Huang et al., 2017). It seems that PPAR and antioxidant enzymes play a role in ERR $\alpha$  regulation of BACE1, either in normal condition or in oxidative stress. However, ERR $\alpha$  regulation of ADAM10 occurs only in oxidative stress. Previous study has demonstrated that while H<sub>2</sub>O<sub>2</sub> increases APP and BACE1 expression, it inhibits ADAM10 (Azmi et al., 2015; Nagai et al., 2017). The reduced ADAM10 expression may have been reversed through antioxidant activity of ERR $\alpha$  (Deblois et al., 2009; Rangwala et al., 2007).

Our study also highlights an important role of ERR $\alpha$  in Tau phosphorylation. It is reported that deregulation of Tau at Ser262, Thr231, and Ser396 is closely associated with oxidative stress and AD pathology (Lee and Leugers, 2012; Mondragon-Rodriguez et al., 2013). Interestingly, these sites can be regulated by GSK3 $\beta$ , which also plays a key role in AD (Hanger and Noble, 2011; Llorens-Martin et al., 2014). In our study, overexpression of ERR $\alpha$  sharply decreases the level of p-Tau262 and p-Tau396, whereas p-Tau231 remains unchanged. These changes may be attributed, in part, to the concomitant decrease of p-GSK3 $\beta$  level in ERR $\alpha$  overexpressing cells (Fig. 5C&D). Although evidence showing that p-GSK3 $\beta$  is directly inhibited by ERR $\alpha$  is lacking, it is reported that ERR $\alpha$  may act against ERR $\gamma$  (Audet-Walsh and Giguere, 2015; Eichner et al., 2010), an isoform of ERR $\alpha$ , which promotes GSK3 $\beta$  phosphorylation (Lim et al., 2015). However, the unchanged p-Tau231 in ERR $\alpha$  overexpressing cells suggests that mechanisms other than GSK3 $\beta$  may also play a role. It is reported that p-Tau231 can be regulated by other kinases including AMP-activated protein kinase (AMPK) (Wang et al., 2013). In muscle cells, downregulation of ERR $\alpha$  is associated with enhanced AMPK activation (LaBarge et al., 2014), suggesting that AMPK may act against ERR $\alpha$  in Thr231 phosphorylation, leading to the unchanged level of p-Tau231.

In summary, we describe the expression pattern of ERR $\alpha$  in APP/PS1 mice. We further show that ERR $\alpha$  inhibits amyloidogenesis and Tau phosphorylation at selective sites, which is preserved in oxidative stress. These results support previous findings that antioxidant reduces A $\beta$  generation and Tau phosphorylation (Murakami et al., 2011). We propose that ERR $\alpha$  may serve as novel target for AD treatment, which may deserve further study.

## Acknowledgments

This work was supported by the National Natural Science Foundation of China (81220108010) to G-J Chen. We sincerely thank Teng Wang at the Second Affiliated Hospital of Chongqing Medical University for providing instructions with the research.

## References

- Audet-walsh, É., Giguère, V., 2014. The multiple universes of estrogen-related receptor  $\alpha$  and  $\gamma$  in metabolic control and related diseases. *Acta Pharmacol. Sin.* 36, 51–61.
- Audet-Walsh, E., Giguere, V., 2015. The multiple universes of estrogen-related receptor  $\alpha$  and  $\gamma$  in metabolic control and related diseases. *Acta Pharmacol. Sin.* 36, 51–61.
- Azmi, N.H., Ismail, M., Ismail, N., Imam, M.U., Alitheen, N.B., Abdullah, M.A., 2015. Germinated brown rice alters abeta(1-42) aggregation and modulates Alzheimer's disease-related genes in differentiated human SH-SY5Y cells. *Evid. Based Complement. Alternat. Med.* 2015, 153684.
- Ballard, C., Gauthier, S., Corbett, A., Brayne, C., Aarsland, D., Jones, E., 2011. Alzheimer's disease. *Lancet* 377, 1019–1031.
- Banse, H.E., Frank, N., Kwong, G.P., McFarlane, D., 2015. Relationship of oxidative stress in skeletal muscle with obesity and obesity-associated hyperinsulinemia in horses. *Can. J. Vet. Res.* 79, 329–338.
- Bergkessel, M., Guthrie, C., 2013. Colony PCR. *Methods Enzymol.* 529, 299–309.
- Bilkei-Gorzo, A., 2014. Genetic mouse models of brain ageing and Alzheimer's disease. *Pharmacol. Ther.* 142, 244–257.
- Billingsley, M.L., Kincaid, R.L., 1997. Regulated phosphorylation and dephosphorylation

- of tau protein: effects on microtubule interaction, intracellular trafficking and neurodegeneration. *Biochem. J.* 323 (Pt 3), 577–591.
- Blalock, E.M., Chen, K.C., Sharrow, K., Herman, J.P., Porter, N.M., Foster, T.C., Landfield, P.W., 2003. Gene microarrays in hippocampal aging: statistical profiling identifies novel processes correlated with cognitive impairment. *J. Neurosci.* 23, 3807–3819.
- Cabre, R., Jove, M., Naudi, A., Ayala, V., Pinol-Ripoll, G., Gil-Villar, M.P., Dominguez-Gonzalez, M., Obis, E., Berdun, R., Mota-Martorell, N., Portero-Otin, M., Ferrer, I., Pamplona, R., 2016. Specific metabolomics adaptations define a differential regional vulnerability in the adult human cerebral cortex. *Front. Mol. Neurosci.* 9, 138.
- Cao, G., Su, P., Zhang, S., Guo, L., Zhang, H., Liang, Y., Qin, C., Zhang, W., 2016. Ginsenoside Re reduces Abeta production by activating PPARgamma to inhibit BACE1 in N2a/APP695 cells. *Eur. J. Pharmacol.* 793, 101–108.
- Chami, L., Checler, F., 2012. BACE1 is at the crossroad of a toxic vicious cycle involving cellular stress and beta-amyloid production in Alzheimer's disease. *Mol. Neurodegener.* 7, 52.
- Choi, Y.K., Park, J.H., Baek, Y.Y., Won, M.H., Jeoung, D., Lee, H., Ha, K.S., Kwon, Y.G., Kim, Y.M., 2016. Carbon monoxide stimulates astrocytic mitochondrial biogenesis via L-type Ca<sup>2+</sup> channel-mediated PGC-1 $\alpha$ /ERR $\alpha$  activation. *Biochem. Biophys. Res. Commun.* 479, 297–304.
- Cui, H., Moore, J., Ashimi, S.S., Mason, B.L., Drawbridge, J.N., Han, S., Hing, B., Matthews, A., McAdams, C.J., Darbro, B.W., Pieper, A.A., Waller, D.A., Xing, C., Lutter, M., 2013. Eating disorder predisposition is associated with ESRR $\alpha$  and HDAC4 mutations. *J. Clin. Invest.* 123, 4706–4713.
- Cui, H., Lu, Y., Khan, M.Z., Anderson, R.M., McDaniel, L., Wilson, H.E., Yin, T.C., Radley, J.J., Pieper, A.A., Lutter, M., 2015. Behavioral disturbances in estrogen-related receptor  $\alpha$ -null mice. *Cell Rep.* 11, 344–350.
- Deblois, G., Hall, J.A., Perry, M.C., Laganieri, J., Ghahremani, M., Park, M., Hallett, M., Giguere, V., 2009. Genome-wide identification of direct target genes implicates estrogen-related receptor  $\alpha$  as a determinant of breast cancer heterogeneity. *Cancer Res.* 69, 6149–6157.
- Eichner, L.J., Perry, M.C., Dufour, C.R., Bertos, N., Park, M., St-Pierre, J., Giguere, V., 2010. miR-378(\*) mediates metabolic shift in breast cancer cells via the PGC-1 $\beta$ /ERR $\gamma$  transcriptional pathway. *Cell Metab.* 12, 352–361.
- Endres, K., Fahrenholz, F., 2012. Regulation of alpha-secretase ADAM10 expression and activity. *Exp. Brain Res.* 217, 343–352.
- Feng, Y., Xia, Y., Yu, G., Shu, X., Ge, H., Zeng, K., Wang, J., Wang, X., 2013. Cleavage of GSK-3 $\beta$  by calpain counteracts the inhibitory effect of Ser9 phosphorylation on GSK-3 $\beta$  activity induced by H(2)O(2). *J. Neurochem.* 126, 234–242.
- Ferri, C.P., Prince, M., Brayne, C., Brodaty, H., Fratiglioni, L., Ganguli, M., Hall, K., Hasegawa, K., Hendrie, H., Huang, Y., Jorm, A., Mathers, C., Menezes, P.R., Rimmer, E., Sczuzfca, M., 2005. Global prevalence of dementia: a Delphi consensus study. *Lancet* 366, 2112–2117.
- Giguere, V., 2008. Transcriptional control of energy homeostasis by the estrogen-related receptors. *Endocr. Rev.* 29, 677–696.
- Gofflot, F., Chartoire, N., Vasseur, L., Heikkinen, S., Dembele, D., Le Merrer, J., Auwerx, J., 2007. Systematic gene expression mapping clusters nuclear receptors according to their function in the brain. *Cell* 131, 405–418.
- Hanger, D.P., Noble, W., 2011. Functional implications of glycogen synthase kinase-3-mediated tau phosphorylation. *Int. J. Alzheimers Dis.* 2011, 352805.
- Hu, L.T., Zhu, B.L., Lai, Y.J., Long, Y., Zha, J.S., Hu, X.T., Zhang, J.H., Chen, G.J., 2017. HMGC52 promotes autophagic degradation of the amyloid-beta precursor protein through ketone body-mediated mechanisms. *Biochem. Biophys. Res. Commun.* 486, 492–498.
- Huang, T., Liu, R., Fu, X., Yao, D., Yang, M., Liu, Q., Lu, W.W., Wu, C., Guan, M., 2017. Aging reduces an ERR $\alpha$ -directed mitochondrial glutaminase expression suppressing glutamine anaplerosis and osteogenic differentiation of mesenchymal stem cells. *Stem Cells* 35, 411–424.
- Huss, J.M., Kelly, D.P., 2004. Nuclear receptor signaling and cardiac energetics. *Circ. Res.* 95, 568–578.
- Huss, J.M., Garbacz, W.G., Xie, W., 2015. Constitutive activities of estrogen-related receptors: transcriptional regulation of metabolism by the ERR pathways in health and disease. *Biochim. Biophys. Acta* 1852, 1912–1927.
- Hyatt, H.W., Smuder, A.J., Sollanek, K.J., Morton, A.B., Roberts, M.D., Kavazis, A.N., 2016. Comparative changes in antioxidant enzymes and oxidative stress in cardiac, fast twitch and slow twitch skeletal muscles following endurance exercise training. *Int. J. Physiol. Pathophysiol. Pharmacol.* 8, 160–168.
- Jakob-Roetne, R., Jacobsen, H., 2009. Alzheimer's disease: from pathology to therapeutic approaches. *Angew. Chem. Int. Ed. Engl.* 48, 3030–3059.
- El Kadmiri, N., Said, N., Slassi, I., El Moutawakil, B., Nadifi, S., 2017. Biomarkers for Alzheimer disease: classical and novel Candidates' review. *Neuroscience* 370, 181–190.
- LaBarge, S., McDonald, M., Smith-Powell, L., Auwerx, J., Huss, J.M., 2014. Estrogen-related receptor- $\alpha$  (ERR $\alpha$ ) deficiency in skeletal muscle impairs regeneration in response to injury. *FASEB J.* 28, 1082–1097.
- Lee, G., Leugers, C.J., 2012. Tau and tauopathies. *Prog. Mol. Biol. Transl. Sci.* 107, 263–293.
- Lim, J.H., Kim, E.N., Kim, M.Y., Chung, S., Shin, S.J., Kim, H.W., Yang, C.W., Kim, Y.S., Chang, Y.S., Park, C.W., Choi, B.S., 2012. Age-associated molecular changes in the kidney in aged mice. *Oxidative Med. Cell. Longev.* 2012, 171383.
- Lim, J., Choi, H.S., Choi, H.J., 2015. Estrogen-related receptor  $\gamma$  regulates dopaminergic neuronal phenotype by activating GSK3 $\beta$ /NFAT signaling in SH-SY5Y cells. *J. Neurochem.* 133, 544–557.
- Liu, Y., Wang, T., Liu, X., Wei, X., Xu, T., Yin, M., Ding, X., Mo, L., Chen, L., 2017. Neuronal zinc-alpha2-glycoprotein is decreased in temporal lobe epilepsy in patients and rats. *Neuroscience* 357, 56–66.
- Llorens-Martin, M., Jurado, J., Hernandez, F., Avila, J., 2014. GSK-3 $\beta$ , a pivotal kinase

- in Alzheimer disease. *Front. Mol. Neurosci.* 7, 46.
- Ly, P.T., Wu, Y., Zou, H., Wang, R., Zhou, W., Kinoshita, A., Zhang, M., Yang, Y., Cai, F., Woodgett, J., Song, W., 2013. Inhibition of GSK3 $\beta$ -mediated BACE1 expression reduces Alzheimer-associated phenotypes. *J. Clin. Invest.* 123, 224–235.
- Mangialasche, F., Solomon, A., Winblad, B., Mecocci, P., Kivipelto, M., 2010. Alzheimer's disease: clinical trials and drug development. *Lancet Neurol.* 9, 702–716.
- Mistry, N.F., Cresci, S., 2010. PPAR transcriptional activator complex polymorphisms and the promise of individualized therapy for heart failure. *Heart Fail. Rev.* 15, 197–207.
- Mondragon-Rodriguez, S., Perry, G., Zhu, X., Moreira, P.I., Acevedo-Aquino, M.C., Williams, S., 2013. Phosphorylation of tau protein as the link between oxidative stress, mitochondrial dysfunction, and connectivity failure: implications for Alzheimer's disease. *Oxidative Med. Cell. Longev.* 2013, 940603.
- Mootha, V.K., Bunkenborg, J., Olsen, J.V., Hjerrild, M., Wisniewski, J.R., Stahl, E., Bolouri, M.S., Ray, H.N., Sihag, S., Kamal, M., Patterson, N., Lander, E.S., Mann, M., 2003. Integrated analysis of protein composition, tissue diversity, and gene regulation in mouse mitochondria. *Cell* 115, 629–640.
- Murakami, K., Shimizu, T., Irie, K., 2011. Formation of the 42-mer amyloid beta radical and the therapeutic role of superoxide dismutase in Alzheimer's disease. *J. Amino Acids* 2011, 654207.
- Nagai, N., Kotani, S., Mano, Y., Ueno, A., Ito, Y., Kitaba, T., Takata, T., Fujii, N., 2017. Ferulic acid suppresses amyloid beta production in the human lens epithelial cell stimulated with hydrogen peroxide. *Biomed. Res. Int.* 2017 (5343010).
- Pimplikar, S.W., 2009. Reassessing the amyloid cascade hypothesis of Alzheimer's disease. *Int. J. Biochem. Cell Biol.* 41, 1261–1268.
- Postina, R., 2012. Activation of alpha-secretase cleavage. *J. Neurochem.* 120 (Suppl. 1), 46–54.
- Querfurth, H.W., LaFerla, F.M., 2010. Alzheimer's disease. *N. Engl. J. Med.* 362, 329–344.
- Rangwala, S.M., Li, X., Lindsley, L., Wang, X., Shaughnessy, S., Daniels, T.G., Szustakowski, J., Nirmala, N.R., Wu, Z., Stevenson, S.C., 2007. Estrogen-related receptor alpha is essential for the expression of antioxidant protection genes and mitochondrial function. *Biochem. Biophys. Res. Commun.* 357, 231–236.
- Ranhotra, H.S., 2009. Up-regulation of orphan nuclear estrogen-related receptor alpha expression during long-term caloric restriction in mice. *Mol. Cell. Biochem.* 332, 59–65.
- Ranhotra, H.S., 2015a. Estrogen-related receptor alpha and mitochondria: tale of the titans. *J. Recept. Signal Transduct. Res.* 35, 386–390.
- Ranhotra, H.S., 2015b. The orphan estrogen-related receptor alpha and metabolic regulation: new frontiers. *J. Recept. Signal Transduct. Res.* 35, 565–568.
- Sheng, B., Wang, X., Su, B., Lee, H.G., Casadesus, G., Perry, G., Zhu, X., 2012. Impaired mitochondrial biogenesis contributes to mitochondrial dysfunction in Alzheimer's disease. *J. Neurochem.* 120, 419–429.
- Singer, O., Marr, R.A., Rockenstein, E., Crews, L., Coufal, N.G., Gage, F.H., Verma, I.M., Masliah, E., 2005. Targeting BACE1 with siRNAs ameliorates Alzheimer disease neuropathology in a transgenic model. *Nat. Neurosci.* 8, 1343–1349.
- Strum, J.C., Shehee, R., Virley, D., Richardson, J., Mattie, M., Selley, P., Ghosh, S., Nock, C., Saunders, A., Roses, A., 2007. Rosiglitazone induces mitochondrial biogenesis in mouse brain. *J. Alzheimers Dis.* 11, 45–51.
- Tamagno, E., Bardini, P., Obbili, A., Vitali, A., Borghi, R., Zaccheo, D., Pronzato, M.A., Danni, O., Smith, M.A., Perry, G., Tabaton, M., 2002. Oxidative stress increases expression and activity of BACE in NT2 neurons. *Neurobiol. Dis.* 10, 279–288.
- Tarrant, A.M., Greytak, S.R., Callard, G.V., Hahn, M.E., 2006. Estrogen receptor-related receptors in the killifish *Fundulus heteroclitus*: diversity, expression, and estrogen responsiveness. *J. Mol. Endocrinol.* 37, 105–120.
- Wang, J.Z., Xia, Y.Y., Grundke-Iqbal, I., Iqbal, K., 2013. Abnormal hyperphosphorylation of tau: sites, regulation, and molecular mechanism of neurofibrillary degeneration. *J. Alzheimers Dis.* 33 (Suppl. 1), S123–139.
- Wang, S., Dougherty, E.J., Danner, R.L., 2016. PPAR $\gamma$  signaling and emerging opportunities for improved therapeutics. *Pharmacol. Res.* 111, 76–85.
- Webster, S.J., Bachstetter, A.D., Nelson, P.T., Schmitt, F.A., Van Eldik, L.J., 2014. Using mice to model Alzheimer's dementia: an overview of the clinical disease and the preclinical behavioral changes in 10 mouse models. *Front. Genet.* 5, 88.
- Yan, R., Fan, Q., Zhou, J., Vassar, R., 2016. Inhibiting BACE1 to reverse synaptic dysfunctions in Alzheimer's disease. *Neurosci. Biobehav. Rev.* 65, 326–340.
- Ye, Q., Chen, C., Si, E., Cai, Y., Wang, J., Huang, W., Li, D., Wang, Y., Chen, X., 2017. Mitochondrial effects of PGC-1 $\alpha$  silencing in MPP(+)-treated human SH-SY5Y neuroblastoma cells. *Front. Mol. Neurosci.* 10, 164.
- Yuk, J.M., Kim, T.S., Kim, S.Y., Lee, H.M., Han, J., Dufour, C.R., Kim, J.K., Jin, H.S., Yang, C.S., Park, K.S., Lee, C.H., Kim, J.M., Kweon, G.R., Choi, H.S., Vanacker, J.M., Moore, D.D., Giguere, V., Jo, E.K., 2015. Orphan nuclear receptor ERR $\alpha$  controls macrophage metabolic signaling and A20 expression to negatively regulate TLR-induced inflammation. *Immunity* 43, 80–91.
- Zhou, X., Chen, M., Zeng, X., Yang, J., Deng, H., Yi, L., Mi, M.T., 2014. Resveratrol regulates mitochondrial reactive oxygen species homeostasis through Sirt3 signaling pathway in human vascular endothelial cells. *Cell Death Dis.* 5, e1576.
- Zhu, B., Zha, J., Long, Y., Hu, X., Chen, G., Wang, X., 2016. Increased expression of copine VI in patients with refractory epilepsy and a rat model. *J. Neurol. Sci.* 360, 30–36.